Stability of Supported Amine Adsorbents to SO2 and NOx in Postcombustion CO2 Capture. 1. Single-Component Adsorption

ARTICLE *in* INDUSTRIAL & ENGINEERING CHEMISTRY RESEARCH · AUGUST 2013

Impact Factor: 2.59 · DOI: 10.1021/ie4019116

2 AUTHORS, INCLUDING:

Fateme Rezaei
Missouri University of Science and Technology
45 PUBLICATIONS **542** CITATIONS

SEE PROFILE

I&EC research
Industrial & Engineering Chemistry Research

Article

pubs.acs.org/IECR

Stability of Supported Amine Adsorbents to SO_2 and NO_x in Postcombustion CO_2 Capture. 1. Single-Component Adsorption

Fateme Rezaei and Christopher W. Jones*

School of Chemical & Biomolecular Engineering, Georgia Institute of Technology, 311 Ferst Drive, Atlanta, Georgia 30332, United States

ABSTRACT: Flue gases from coal-fired power plants typically contain not only CO_2 but other acid-gas impurities such as SO_x and NO_x that can dramatically influence the CO_2 capture efficiency. Whereas postcombustion CO_2 capture by aminosilica materials has been extensively studied over the past few years because of their high equilibrium CO_2 capacities, the performance of these materials under realistic conditions (in the presence of SO_x, NO_x, and O_2) remains relatively unexplored. In this study, the degree of irreversible binding of SO_2, NO, and NO_2 to four supported amine adsorbents is evaluated to assess the SO_2, NO, and NO_2 adsorption capacities of aminosilica sorbents and their effects on the CO_2 adsorption capacities. Adsorbents constructed using poly(ethyleneimine) and three different silane coupling agents (based on propyltrimethoxysilane linkers) with primary, secondary, and tertiary amines are evaluated. Under the experimental conditions used in this investigation, it is found that primary amines with high amine loadings displayed more affinity toward NO than their secondary and tertiary amine counterparts. However, overall, NO adsorption on the aminosilica adsorbents is low, and therefore, the CO_2 capacities of the adsorbent materials exposed to NO remained almost unchanged after the exposure. In contrast, all materials showed a very high nitrogen dioxide adsorption capacity upon exposure to NO_2. As a result, all adsorbents treated with NO_2 exhibited a dramatic reduction in CO_2 capacity, which corresponds to the deactivation of amine groups due to the irreversible binding of NO_2. In addition, our results indicate that SO_2 adsorbed significantly on supported amine adsorbents, resulting in a dramatic loss in CO_2 capacity during CO_2 capture from flue gas. With similar amine loadings, although secondary amines exhibited higher affinity to SO_2, their CO_2 capacity loss after exposure to SO_2 is lower than that of primary amines, indicating that these materials are more stable in the presence of SO_2, which implies that more SO_2 desorbs from secondary amines during the desorption step. These results suggest that for silica-supported amine materials to be useful in practical CO_2 capture applications, it is necessary to significantly reduce the SO_2 and NO_2 concentrations of the flue gas prior to the CO_2 capture process. On the other hand, the capture efficiency of these materials does not change significantly in the presence of NO. This suggests that such materials might be promising for postcombustion CO_2 capture from flue gas streams derived from natural gas combustion, as these streams typically contain reduced SO_2 concentrations but can still have significant NO_x concentrations.

1. INTRODUCTION

Many researchers around the world have studied carbon capture and sequestration as a means to slow the rate of increase of CO_2 in the atmosphere, with the main focus being placed on postcombustion CO_2 capture applications.[1,2] Solid adsorbents have gained a great deal of attention as potential candidates for practical carbon capture. These solid adsorbents include, but are not limited to, zeolites, activated carbons, activated alumina, metal oxides, ion-exchange resins, metal−organic frameworks, and organic−inorganic hybrids such as silica-supported amine adsorbents.[3,4] Among the array of available solid adsorbents, supported amine materials have been extensively studied in recent years because of the many advantages offered by this class of adsorbents compared to other solid adsorbents. These advantages include high CO_2 equilibrium capacities, fast adsorption kinetics,[5] high efficiency in humid conditions, and ease of regeneration.[3,9] This array of adsorbents has been previously classified into three groups:[9,10] class 1 adsorbents that are based on the physical impregnation of silica support with amine-containing polymers; class 2 adsorbents that are based on the grafting of organosilanes to the surface of the silica; and finally, class 3 materials that are prepared by the in situ polymerization of amine-containing monomers on and in the silica support.

The majority of the literature on supported amine adsorbents is focused solely on the development of adsorbents with good (mostly equilibrium) CO_2 capacities.[9] Comparatively little work has been done on the stability of supported amine adsorbents in the presence of flue gas impurities such as SO_x, NO_x, oxygen, and steam.[11] In fact, these impurities cause a number of practical issues in CO_2 capture processes, including decreased adsorbent lifetime and capacity, adsorbent poisoning, low product purity, and increased operating costs. For widespread deployment of CO_2 capture systems, all of these difficulties will need to be addressed. The typical concentrations of SO_x and NO_x in coal-fired power plants (before sulfur scrubbing and/or selective catalytic reaction units) are approximately 0.2−0.25 and 0.15−0.2 vol %, respectively, whereas the approximate CO_2 concentrations in similar power stations are 9−14 vol %.[17]

Supported amine adsorbents have gained increased attention for flue gas capture because of their inherent high adsorption

Received: June 17, 2013
Revised: July 25, 2013
Accepted: July 25, 2013
Published: July 25, 2013

dx.doi.org/10.1021/ie4019116 | *Ind. Eng. Chem. Res.* 2013, 52, 12192−12201

capacities.[9] However, these solid-supported amines are susceptible to poisoning by flue gas contaminants such as SO_x and NO_x impurities, just as the liquid amine media are affected. SO_x and NO_x have been shown to bind irreversibly to most amine groups;[16,18,19,21−23] therefore, competitive adsorption of SO_x/NO_x on amine adsorbents needs to be addressed. Diaf et al. and Diaf and Beckman studied the adsorption of weakly acidic gases such as CO_2, SO_2, NO_2, and NO onto amine-containing polymeric adsorbents and investigated the effects of amine structure on acid-gas sorption and thermal reversibility of the sorption−desorption reactions.[16,18] They found that the thermal reversibility of the capture process decreased in the order $CO_2 > SO_x > NO_x$. They also showed that, although tertiary-amine-functional copolymers exhibited a rather poor CO_2 adsorption capacity, such polymers have a high affinity for Lewis acid gases stronger than CO_2 (SO_2, for instance). In another study, conducted by Xu et al., the adsorption separation performance and the stability of a class 1, "molecular basket" adsorbent made of PEI-impregnated MCM-41 was studied in the presence of 60−70 ppm NO_x and 200−300 ppm CO.[19] They showed that the adsorbent simultaneously adsorbed CO_2 and NO_x. Although the amount of CO_2 adsorbed was significantly higher than the amount of NO_x, very little NO_x desorbed during the desorption step, indicating the irreversible adsorption of NO_x. In a study performed by Chuang and co-workers, the SO_2 adsorption capacity of amine-grafted SBA-15 (a class 2 material) and its influence on the CO_2 adsorption capacity were evaluated, and the results revealed that the SO_2 that was adsorbed irreversibly onto the material blocked some amine sites toward subsequent CO_2 adsorption, hence reducing the CO_2 adsorption capacity.[17] Belmabkhout and Sayari studied the SO_2 desorption performance of triamine-functionalized pore-expanded MCM-41 by exposing the material to 0.23 mbar pure SO_2. Their results indicated that only 85% of SO_2 desorbs during desorption at 100 °C under vacuum.[24] In another study conducted by Liu et al., the CO_2 adsorption performance of tetraethylenepentamine (TEPA) functionalized KIT-6 silica (class 1) was evaluated in the presence of SO_2 and NO gas impurities. They found that the CO_2 capacity of their adsorbent changed slightly when it was exposed to SO_2 at concentrations lower than 300 ppm, whereas the material retained its capacity in the presence of NO (below 400 ppm). The material showed stability (i.e., retained its CO_2 adsorption capacity) after 10 cycles at 120 °C.[20]

The adsorption and desorption of SO_x/NO_x gases has also been studied on other solid adsorbent materials such as activated carbon; hydrophobic zeolites such as NaX, ZSM-5, and activated carbon fiber;[25−30] and calcium-based adsorbents.[31−34] Zhang et al. studied the effect of flue gas impurities such as O_2, SO_x, NO_x, and water on the CO_2 capture performance of alumina and NaX zeolite by vacuum swing adsorption.[35] They reported a very slow SO_2 desorption from these materials mainly because of their large capacity and strong chemical adsorption, whereas, NO desorption occurred fairly quickly.

As noted earlier, the stability to SO_2 and NO_x of any adsorbents targeted for postcombustion CO_2 capture applications will be critical in determining the lifetime of the adsorbents and in turn, the viability of processes based on such adsorbents for practical application. Although it is known that these gases adsorb onto supported amine adsorbents, relatively little quantitative information has been published on the effect of these gases on amine adsorbents with different structures, and thus, this study focuses on the effects of these contaminants on an array of specific, well-defined supported amine powders. Specifically, in this work, we systematically explored the stabilities and CO_2 adsorption capacities of a series of well-defined, class 2 amine adsorbents[9] containing only primary, secondary, and tertiary amines in the presence of SO_2 and NO_x. In parallel, class 1 adsorbents based on PEI impregnated on the same support were evaluated. The degree of irreversible binding of SO_2, NO, and NO_2 to the supported amine adsorbents after exposure at concentrations relevant to CO_2 capture was evaluated. To understand the interaction effects of SO_2 and NO_x on CO_2 adsorption, coadsorption experiments should be performed, which will be the focus of future work.

2. EXPERIMENTAL SECTION

2.1. Materials Synthesis. The commercial silica PD09024, from PQ Corporation, was used to synthesize the supported amine adsorbents. The standard class 1 adsorbents (PEI-based materials) were synthesized using a conventional wet impregnation method. First, the desired amount of PEI was dissolved in methanol for 1 h, dried silica was then added, and the mixture was stirred for an additional 12 h. The methanol solvent was later removed by a rotary evaporator, and the resulting adsorbent was further dried under a vacuum at 105 °C overnight before testing. For the preparation of class 2 adsorbents (aminosilane-based materials), the silica was functionalized through the reaction of three different silane coupling agents with surface silanols. First, the desired amounts of toluene and silica were mixed for 1 h, and then the desired amount of silane was added. The mixture was kept under vigorous stirring for 24 h at 85 °C. The resulting adsorbent was recovered by filtration, washed with toluene, and then dried under a vacuum at 105 °C. Adsorbents with different amine loadings were prepared for each material type. Table 1 summarizes the materials used to synthesize supported amine adsorbents and their corresponding nomenclature.

Table 1. Amine Materials Used to Prepare Aminosilica Adsorbents

amine	amine type(s)	sample name
poly(ethyleneimine)	primary, secondary, tertiary: PEI	PD-PEI_2
		PD-PEI_4
		PD-PEI_8
3-aminopropyltrimethoxysilane	primary: APS	PD-APS_1
		PD-APS_2
		PD-APS_4
(*N*-methylaminopropyl) trimethoxysilane	secondary: MAPS	PD-MAPS_1
		PD-MAPS_2
(*N*,*N*-dimethylaminopropyl) trimethoxysilane	tertiary: DMAPS	PD-DMAPS_1
		PD-DMAPS_2

2.2. Materials Characterization. Nitrogen physisorption measurements were carried out on a Micromeritics TRISTAR II instrument at 77 K. Surface areas and pore volumes were calculated from the collected isotherm data. Surface areas were calculated using the Brunauer−Emmett−Teller (BET) method, and pore volumes and pore diameters were calculated using the Broekhoff−de Boer method with the Frenkel−Halsey−Hill equation (BdB−FHH method).[36] A Netzsch STA409PG thermogravimetric analysis (TGA) apparatus was used to determine the organic loading of the materials. ^{13}C cross-

polarization magic-angle-spinning (CP-MAS) solid-state nuclear magnetic resonance (NMR) measurements were carried out on a Bruker DSX-300 spectrometer. The samples were spun at a frequency of 10 kHz, and 15000 scans were obtained. Fourier transform infrared (FT-IR) and FT-Raman spectroscopy measurements were performed on a Bruker Vertex 80v optical bench.

2.3. Single-Component Adsorption Measurements. The single-component adsorptions of CO_2, SO_2, NO, and NO_2 onto supported amine adsorbents were carried out using a Q500 thermogravimetric analyzer (TA Instruments) by directly exposing the material to inert-gas-diluted gas mixtures. For CO_2 adsorption experiments, the materials were first regenerated in flowing helium at 110 °C for 30 min and then exposed to 10% CO_2/He. For SO_2 or NO adsorption experiments, nitrogen was used as a purge gas. The materials were first regenerated in a N_2 flow at 110 °C for 30 min and then separately exposed to SO_2, NO, and NO_2 gases balanced with N_2. The treated adsorbents were again regenerated in a manner similar to that already described. The materials were then used after regeneration for subsequent CO_2 adsorption experiments, following the described procedure, to evaluate their remaining CO_2 capacities after exposure to SO_x/NO_x. For all experiments, the gas flow rate was set to 90 mL/min. To evaluate the degree of irreversible binding of SO_2, three different SO_2 concentrations relevant to postcombustion capture were used, namely, 20, 100, and 200 ppm. For NO and NO_2 gases, only a concentration of 200 ppm was considered. The adsorbents were exposed to the specified gases at three different temperatures: 35, 55, and 75 °C.

3. RESULTS AND DISCUSSION

3.1. Physical Properties of Materials. Table 2 reports the physical characteristics of the bare silica support and amine-functionalized silica adsorbents used in this study, along with the amine loadings of the materials, as determined by TGA. To enable direct comparisons between the adsorption characteristics of the samples, materials were synthesized with similar amine loadings. Two materials with higher loadings of PEI and APS were also synthesized so that the influence of loading on amine efficiency could be assessed. As can be seen in the table, incorporating amines into the pores of the silica supports reduced both the surface areas and the pore volumes, as expected. The amine loadings of the as-synthesized materials are also listed in Table 2.

Table 2. Physical Properties of Amine-Functionalized Silica Adsorbents

material	abbreviation	amine loading (mmol N/g)	S_{BET} (m^2/g)	V_{ppre} (cm^3/g)
silica, bare	PD	–	294	1.04
silica with PEI, low loading	PD-PEI_2	2.1	247	0.76
silica with PEI, medium loading	PD-PEI_4	4.2	202	0.52
silica with PEI, high loading	PD-PEI_8	8.4	78	0.38
silica with APS, low loading	PD-APS_1	1.3	227	0.74
silica with APS, medium loading	PD-APS_2	1.9	213	0.63
silica with APS, high loading	PD-APS_4	3.7	57	0.22
silica with MAPS, low loading	PD-MAPS_1	1.3	255	0.75
silica with MAPS, high loading	PD-MAPS_2	2.1	150	0.50
silica with DMAPS, low loading	PD-DMAPS_1	1.3	250	0.78
silica with DMAPS, high loading	PD-DMAPS_2	1.9	211	0.55

3.2. Adsorption Capacity Measurements. *3.2.1. SO_2 Adsorption: Effect of SO_2 Concentration.* Figure 1a shows the SO_2 adsorption capacities of different adsorbents with comparable amine loadings for exposure to 20, 100, and 200 ppm single-acid-component feed gases at 35 °C. The results indicate that, for all adsorbents, the SO_2 capacities increased significantly with SO_2 concentration. For materials with comparable amine loadings, the MAPS sample containing secondary amines had the highest affinity toward SO_2 at SO_2 concentrations ranging from 20 to 200 ppm. On the other hand, the tertiary amine sorbent (PD-DMAPS_2) displayed the lowest capacity for SO_2. At 20 ppm, the SO_2 capacity of the PD-MAPS_2 material was 0.49 mmol of SO_2/g. With further increases of concentration to 100 and 200 ppm, the adsorption capacity increased to 0.79 and 1.08 mmol of SO_2/g, respectively.

Figure 1b presents the CO_2 adsorption capacities of the SO_2-treated adsorbents normalized by the original adsorption capacities as functions of exposure to SO_2 at different concentrations. With increasing SO_2 concentration, all of the materials experienced an increased CO_2 capacity loss. This is due to the fact that SO_2 adsorbs irreversibly on the surface of the aminosilica adsorbents and, therefore, decreases the available amine sites for subsequent CO_2 adsorption, leading to a loss of CO_2 capacity. It is worth mentioning here that all measurements were performed with dry gases and that the tertiary amine (PD-DMAPS) samples did not appreciably adsorb CO_2 under such conditions.[3,9,37]

3.2.2. SO_2 Adsorption: Effect of Temperature. To verify the effect of temperature on the adsorption performance of the aminosilica materials, the measurements were performed at various adsorption temperatures. The SO_2 adsorption capacities of the aminosilica adsorbents with comparable amine loadings are shown in Figure 2a at three different temperatures (i.e., 35, 55, and 75 °C), and their corresponding CO_2 capacities after the exposure are shown in Figure 2b.

It is evident from these plots that the increase in temperature resulted in a decrease in SO_2 adsorption capacity. The MAPS material with an amine loading of 2.1 mmol of N/g (PD-MAPS_2) displayed a capacity decrease from 1.08 to 0.71 and 0.57 mmol of SO_2/g when the temperature was increased from 35 to 55 and 75 °C, respectively. The DMAPS sample with an amine loading of 1.9 mmol of N/g exhibited an almost negligible SO_2 capacity at elevated temperatures (0.04 mmol of SO_2/g at 75 °C).

Regarding the residual CO_2 capacity, because of the lower affinity toward SO_2 at higher temperatures, the CO_2 capacity was less influenced by exposure to SO_2, and all materials displayed higher normalized CO_2 capacities at 75 °C compared 55 and 35 °C, as shown in Figure 2b. Compared to the PEI- and APS-derived samples, the MAPS adsorbent displayed a higher remaining CO_2 capacity after being exposed to 200 ppm SO_2 at all three temperatures considered here.

3.2.3. SO_2 Adsorption: Effect of Amine Loading. The impact of amine loading on the SO_2 adsorption behavior of the aminosilica adsorbents was also evaluated in this study. Figure

dx.doi.org/10.1021/ie4019116 | Ind. Eng. Chem. Res. 2013, 52, 12192−12201

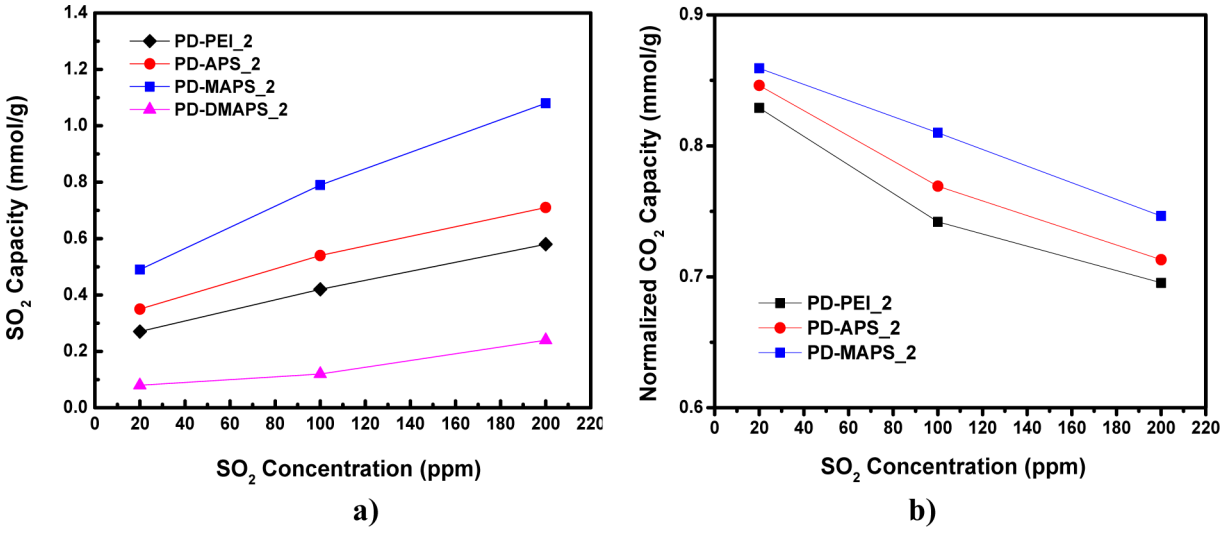

Figure 1. (a) SO_2 adsorption capacities and (b) normalized CO_2 adsorption capacities of aminosilica adsorbents at 35 °C as functions of SO_2 concentration.

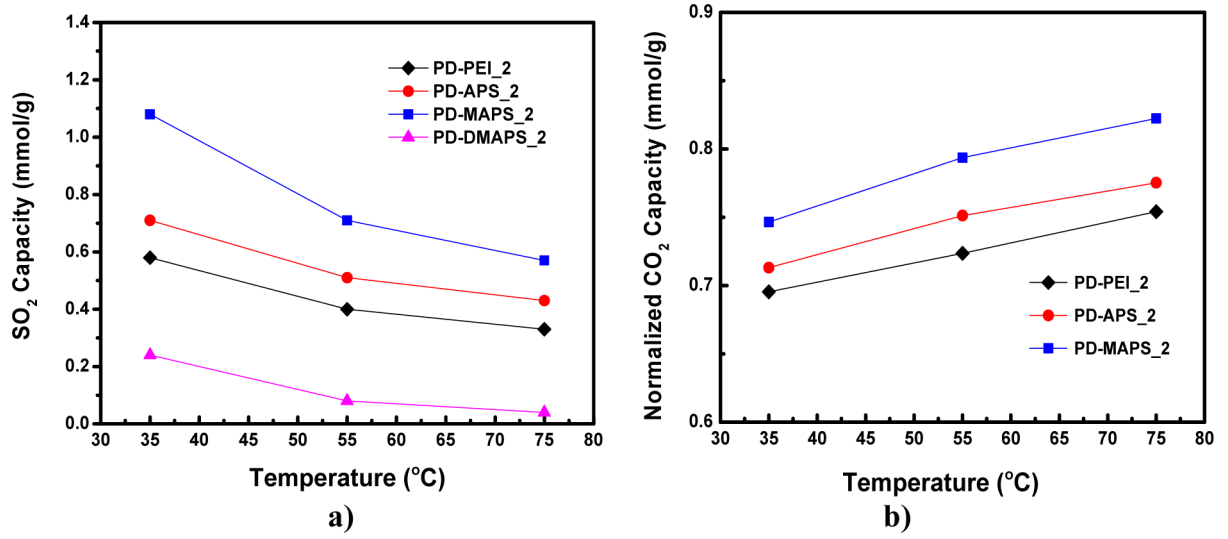

Figure 2. (a) SO_2 adsorption capacities and (b) normalized CO_2 adsorption capacities of aminosilica adsorbents for 200 ppm SO_2 as functions of temperature.

3a shows the SO_2 capacity as a function of amine loading for a 200 ppm gas concentration at a temperature of 35 °C. The bare silica support was also tested by TGA, and it was found that the silica did not appreciably adsorb SO_2 when it was exposed to 200 ppm SO_2 at 35 °C. For the PEI- and APS-based materials, three different amine loadings were used, whereas for the MAPS and DMPAS materials, only two loadings were evaluated. As is evident from this figure, for all materials, the SO_2 equilibrium capacity increased almost linearly with the increase of amine content. The silica-impregnated material (PD-PEI) gave rise to a capacity increase from 0.58 to 1.14 and 2.17 mmol of SO_2/g when the amine loading was increased from 2.1 to 4.2 and 8.4 mmol of N/g, respectively. Additionally, the silica-grafted materials (PD-APS, PD-MAPS, and PD-DMAPS) exhibited the same behavior upon functionalization with higher amine contents.

Figure 3b shows the corresponding amine efficiency of supported amine adsorbents, defined as the number of moles of SO_2 adsorbed per amount of amine (mmol of SO_2/mmol of N). The secondary amine adsorbent with an amine loading of 2.1 mmol of N/g (PD-MAPS_2) displayed the highest amine efficiency (0.51 mmol of SO_2/mmol of N). For all class 2 materials, the amine efficiency increased with amine loading, as in contrast to the class 1 adsorbents, which exhibited a slight decrease in amine efficiency with increased amine loading. The decrease in amine efficiency with PEI content implies that the SO_2 adsorption on PEI-impregnated adsorbents is diffusion-limited when the amine content passes a certain point ($\gtrsim$40%).

3.2.4. Cyclic Experiments. The stability of adsorbent materials in consecutive runs plays a major role in evaluating the overall performance of any hypothetical process, influencing the operating cost. Therefore, it is crucial not only to evaluate the adsorption capacity of materials but also to investigate the material performance under cyclic conditions. Cyclic experiments were therefore performed to evaluate the stability of the materials under cyclic adsorption−desorption conditions. The adsorption measurements were carried out at 35 °C, and the materials were regenerated at 120 °C, over four cycles. The SO_2 and CO_2 adsorption capacities of the two materials that displayed higher capacities to SO_2 (PD-PEI_8 and PD-APS_4)

dx.doi.org/10.1021/ie4019116 | Ind. Eng. Chem. Res. 2013, 52, 12192−12201

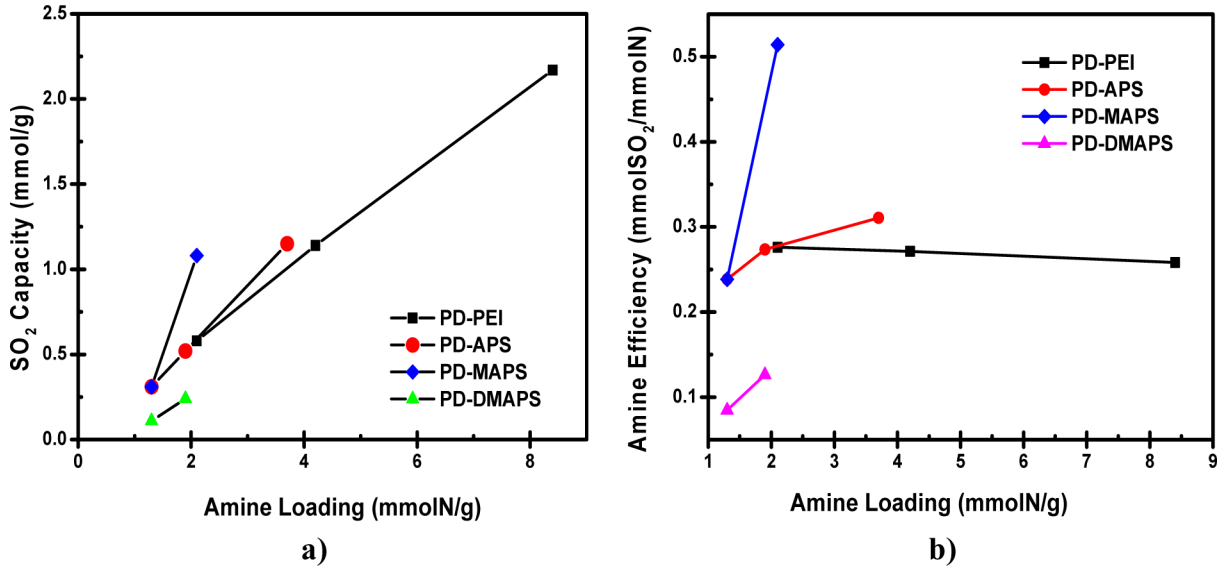

Figure 3. (a) SO_2 adsorption capacity and (b) amine efficiency of aminosilica adsorbents for 200 ppm SO_2 as functions of amine loading at 35 °C.

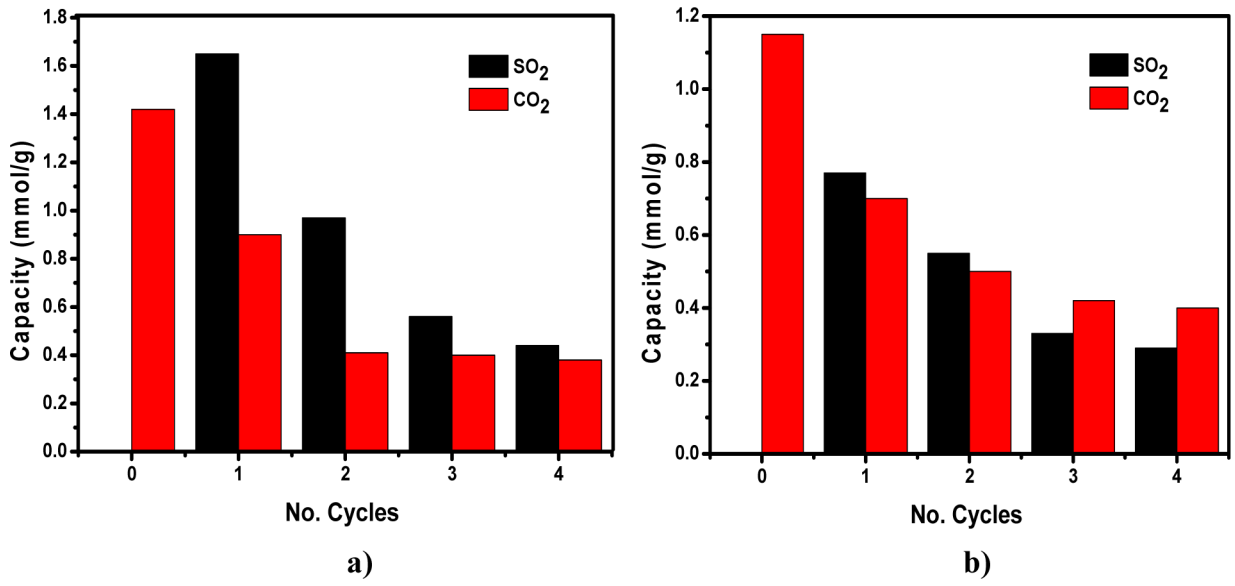

Figure 4. SO_2 and CO_2 adsorption capacities of aminosilica adsorbents over four cycles of adsorption and desorption for (a) PD-PEI_8 and (b) PD-APS_4 at 20 ppm SO_2 and 35 °C.

are presented in Figure 4 for 20 ppm SO_2 and 10% CO_2. The goal here was not to compare their relative performances but rather to study how the materials performed under cyclic tests. Both materials exhibited a dramatic decrease in their SO_2 capacities after the first cycle, from 1.65 to 0.97 mmol of SO_2/g in the case of PD-PEI_8 and from 0.77 to 0.55 mmol of SO_2/g in the case of PD-APS_4. The rate of capacity loss decreased from cycle 2 to cycle 3 for both materials. The same trend was observed for the CO_2 cyclic capacity of the materials over four cycles, showing a fast decrease after the first exposure to SO_2 and a slow decrease after the second cycle, with almost no significant change from cycle 3 to cycle 4. In the case of the PD-PEI_8 adsorbent, the CO_2 capacity decreased dramatically from 1.42 to 0.38 mmol of CO_2/g, and similarly, PD-APS_4 exhibited a dramatic loss in capacity from 1.15 to 0.4 mmol of CO_2/g after four cycles. The trend suggests that, after an initial deactivation period, the adsorbents might enter a phase of somewhat stable operation, although one should be careful in extrapolating results obtained after only four cycles of testing.

3.2.5. NO Adsorption. As flue gas streams coming from coal-fired power plants contain both SO_2 and NO_x impurities, it is important to investigate the NO_x adsorption behavior of the aminosilica materials as well. Figure 5 shows the NO adsorption capacities of the materials for a 200 ppm NO concentration at 35 °C. As can be seen from this figure, except for PD-PEI_8 and PD-APS_4, all of the adsorbents showed very little capacity for NO (all below 0.07 mmol of NO/g). On the contrary, the PEI-impregnated silica adsorbent with an amine content of 8.4 mmol of N/g (PD-PEI_8) and the APS-grafted silica adsorbent with an amine content of 3.7 mmol of N/g gave NO adsorption capacities of 0.35 and 0.22 mmol of NO/g, respectively. Given that these two materials contained primary amines, our results suggest that primary amines adsorb NO much more than their secondary and tertiary counterparts, which is especially evident when the amine loading is high,

dx.doi.org/10.1021/ie4019116 | Ind. Eng. Chem. Res. 2013, 52, 12192−12201

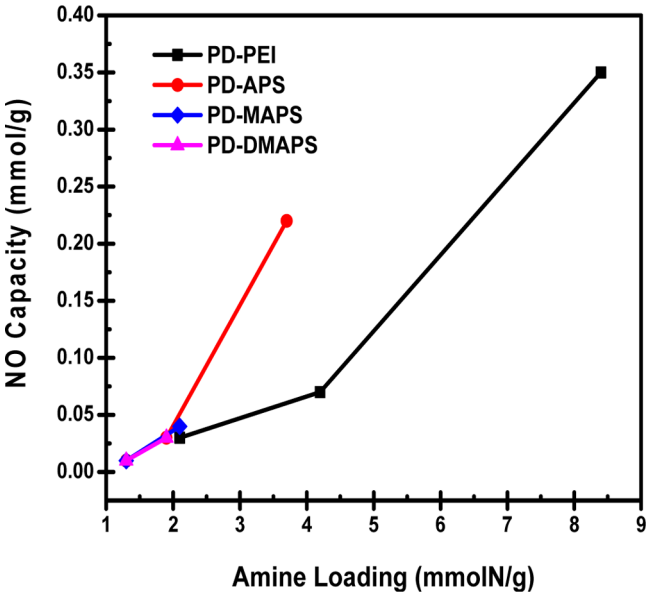

Figure 5. NO adsorption capacities of aminosilica adsorbents for 200 ppm NO at 35 °C.

perhaps indicating a cooperative adsorption involving more than one amine site. Nonetheless, the NO adsorption capacities were all far lower than the corresponding SO_2 adsorption capacities.

The corresponding dry CO_2 capacities before and after NO exposure are displayed in Figure 6. As can be seen from this figure, most materials retained their CO_2 capacity after being exposed to NO, as a result of lower NO adsorption on these materials, as discussed in the preceding paragraph. The data indicate that CO_2 adsorption by secondary and tertiary amines is not significantly influenced by NO and that the capacity loss is less than 5% for these materials. Again, no efficiencies were reported for tertiary amines because their dry CO_2 adsorption was found to be negligible.

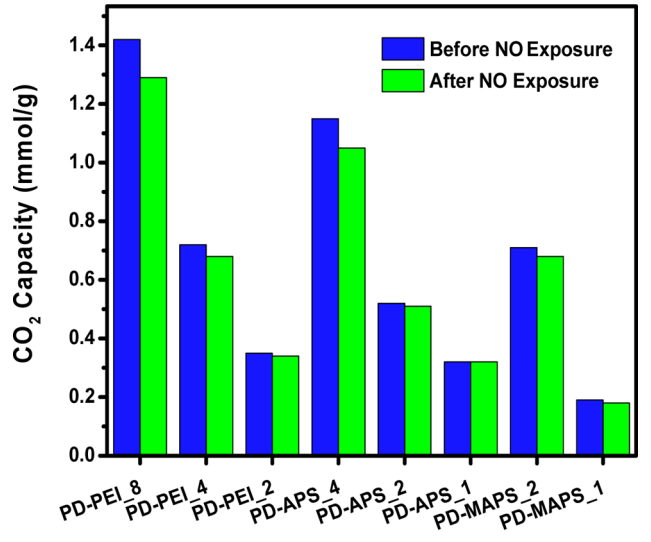

Figure 6. CO_2 capacities of amine-functionalized materials before and after NO exposure.

3.2.6. NO_2 Adsorption. NO_2 is another gaseous compound that is present in flue gas, and although its concentration is not as high as that of NO (NO represents 85–95% of the total NO_x generated in combustion processes),[38] it has previously been shown that NO_2 will bond strongly to some amines and can be irreversibly adsorbed on amine-functionalized materials.[9] To assess the degree of irreversible binding of NO_2, we performed adsorption capacity measurements using 200 ppm NO_2 at 35 °C, and the results are shown in Figure 7. As opposed to NO, NO_2 adsorption on the aminosilica adsorbents examined in this work was found to be very high, and these materials show high affinity toward NO_2. It can be seen that NO_2 adsorbed on the aminosilica adsorbents even more than SO_2 under similar conditions. As with SO_2, the NO_2 capacity increased with amine content for all materials studied here. PD-PEI_8 exhibited the highest uptake, at 3.55 mmol of NO_2/g. For materials with similar amine contents, the secondary amine materials (PD-MAPS) displayed higher NO_2 capacities than the other adsorbents. Surprisingly, the tertiary amine material showed a NO_2 capacity comparable to those of its primary and secondary amine counterparts at both amine loadings.

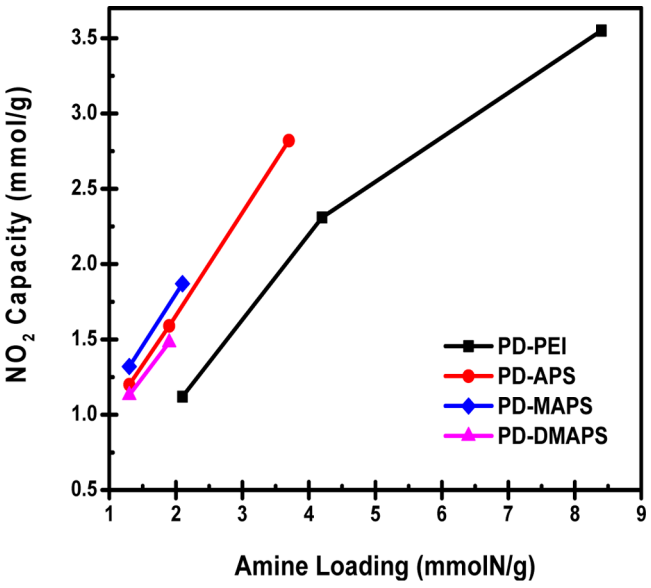

Figure 7. NO_2 adsorption capacities of aminosilica adsorbents for 200 ppm NO_2 at 35 °C.

To probe the effect of NO_2 adsorption on CO_2 adsorption, the CO_2 capacities of the materials were measured before and after exposure to NO_2, and the results are displayed in Figure 8. As a result of their high NO_2 adsorption capacities, the treated materials displayed a significant loss in CO_2 adsorption capacity, indicating that NO_2 was adsorbed irreversibly, reducing the available adsorption sites for CO_2.

3.3. Materials Characterization. *3.3.1. Solid-State NMR Spectroscopy.* The ^{13}C CP-MAS NMR spectra of the adsorbent materials before and after exposure to 200 ppm SO_2 at 35 °C are presented in Figure 9. It is apparent that the PD-APS, PD-MAPS, and PD-DMAPS materials did not show a significant change in chemical structure before and after SO_2 treatment. In contrast, the PD-PEI material treated with 200 ppm SO_2 clearly showed the appearance of a broad peak between 30 and 70 ppm, emerging from overlapping of the individual peaks in the spectrum of the fresh material. For the fresh PD-PEI_8 adsorbent, the peaks at 41.2, 49.8, and 52.1 ppm are attributed to methylene groups adjacent to primary,

dx.doi.org/10.1021/ie4019116 | Ind. Eng. Chem. Res. 2013, 52, 12192–12201

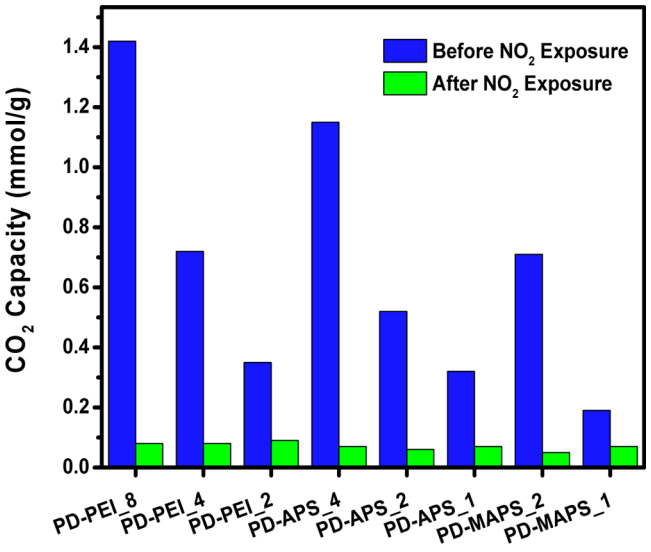

Figure 8. CO_2 capacities of amine-functionalized materials before and after NO_2 exposure.

secondary, and tertiary amines. In the case of PD-APS_4, both fresh and SO_2-treated samples exhibited three peaks at 11.7, 23.1, and 44.7 ppm that correspond to the three carbons in the propyl chain. The three shifts at 11.3, 21.6, and 53.9 ppm for PD-MAPS_2 materials and 11.7, 22.6, and 63.1 ppm for PD-DMAPS_2 samples also indicate the presence of the propyl carbon group. The two materials had an additional shift, at 35.1 and 45.7 ppm, respectively, that corresponds to the methyl group bonded to the amine. For all samples except PD-DMAPS, a new peak emerged at 170 ppm, corresponding to a C═O stretch from CO_2 capture from ambient air.[39]

3.3.2. FT-IR and FT-Raman Spectroscopies. All materials with high amine contents were analyzed before and after treatment with SO_2, NO, and NO_2 using FT-Raman and FT-IR spectroscopies to assess any chemical changes in the surface functional groups. Figure 10 shows the FT-Raman spectra of the fresh and SO_2-, NO-, and NO_2-treated adsorbents. In all FT-Raman spectra, the C—H stretching peaks in the 2700–3100 cm^{-1} range from all of the adsorbents showed essentially no change after exposure to SO_2, NO, and NO_2, indicating that the majority of the CH_2 groups were stable in the presence of these impurity gases. Whereas the Raman spectra of the fresh and NO-treated samples revealed no distinct differences in chemical structure because of the low adsorption of this gas, the SO_2-treated PD-PEI and PD-APS materials revealed two bands in their FT-Raman spectra at 1050 and 690 cm^{-1} that correspond to S═O and S—O stretching vibrations, respectively. This might be due to the formation of sulfates and/or sulfites on the surface of adsorbents when they are exposed to SO_2. Also noteworthy in the spectra of the materials

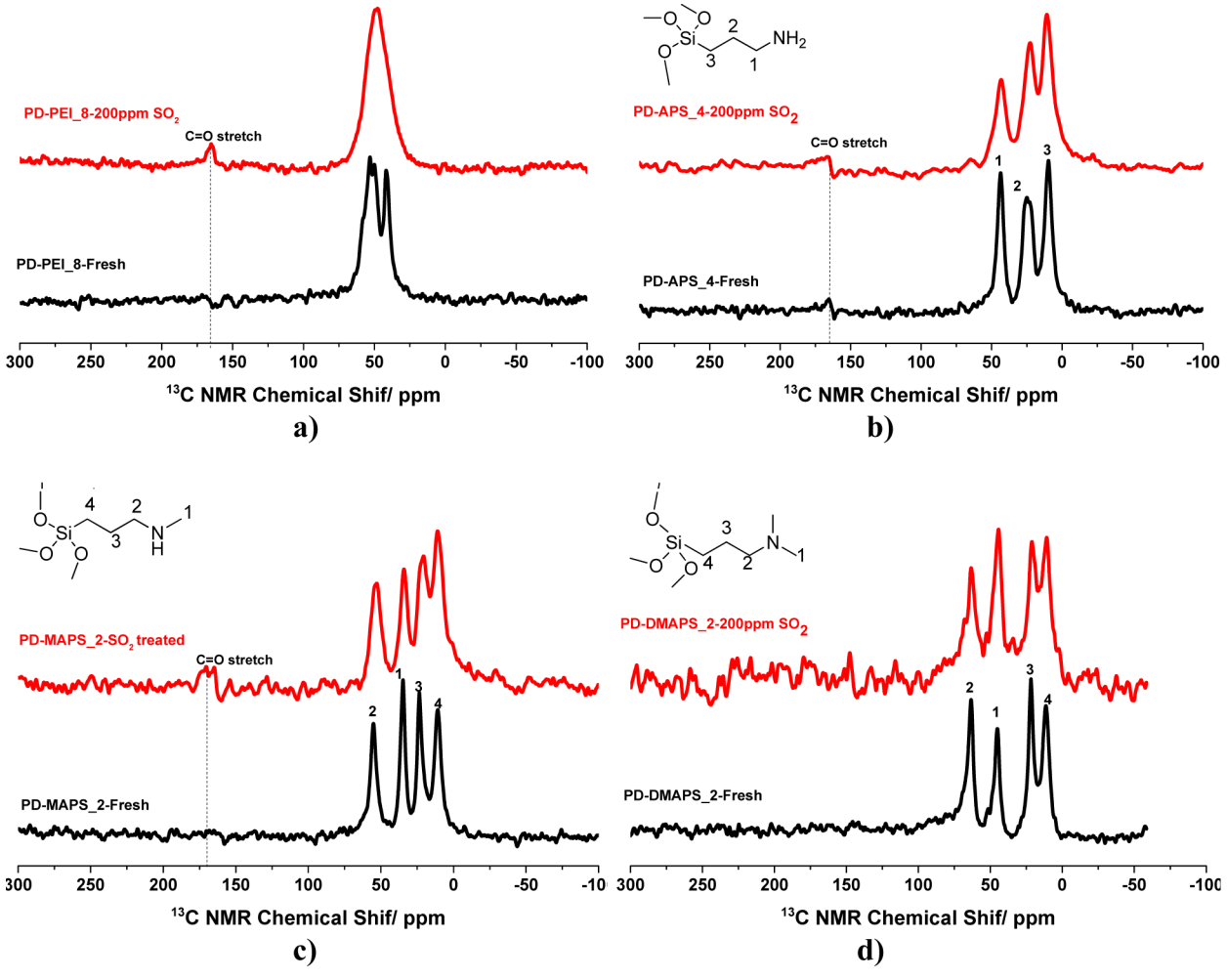

Figure 9. ^{13}C NMR spectra for (a) PEI, (b) APS, (c) MAPS, and (d) DMAPS before and after exposure to 200 ppm SO_2 at 35 °C.

dx.doi.org/10.1021/ie4019116 | Ind. Eng. Chem. Res. 2013, 52, 12192–12201

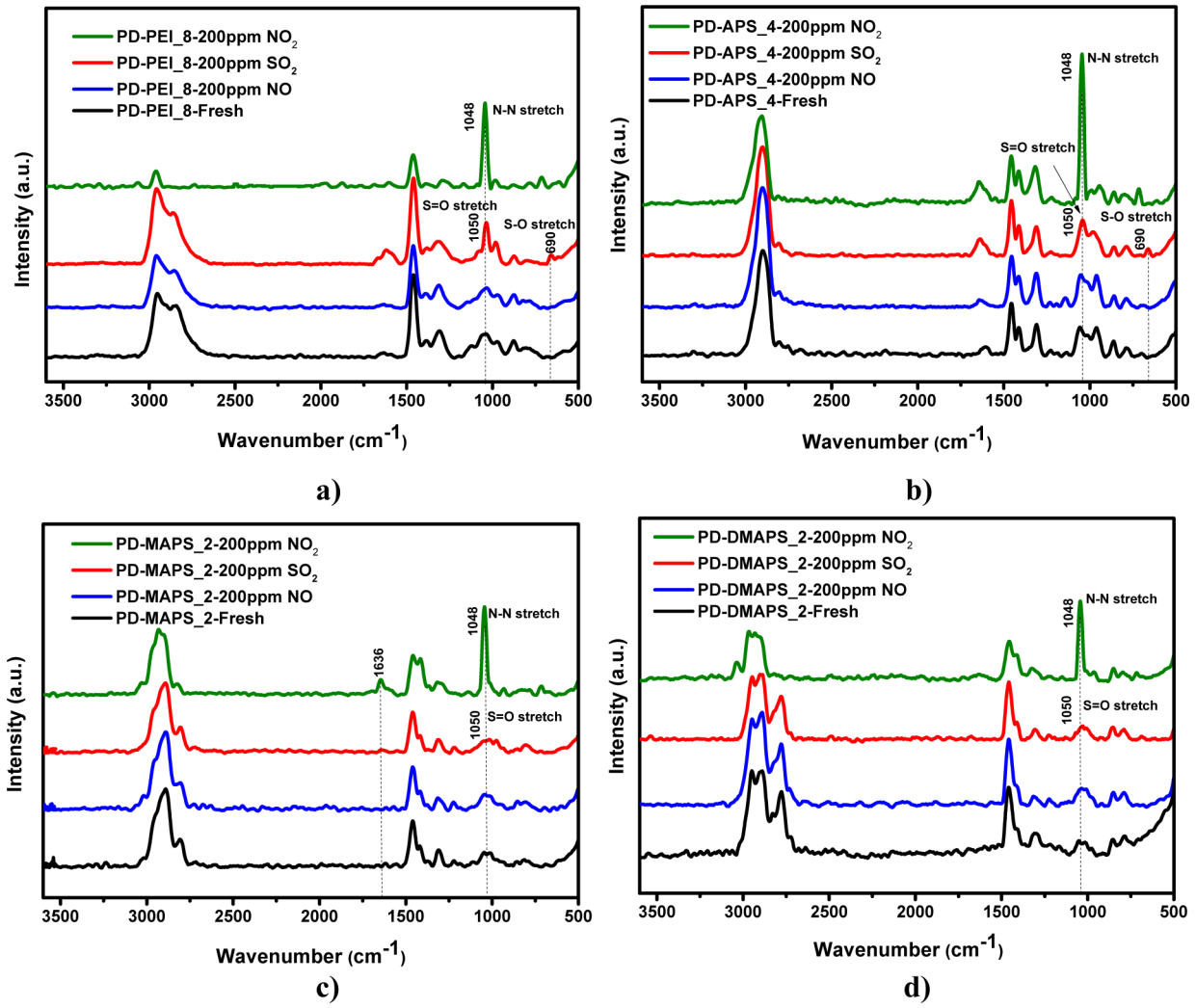

Figure 10. FT-Raman spectra of (a) PEI, (b) APS, (c) MAPS, and (d) DMAPS before and after exposure to 200 ppm SO_2, NO_2, and NO at 35 °C.

exposed to NO_2 is the appearance of the 1048 cm^{-1} band that corresponds to N—N symmetric stretching modes due to the presence of nitrate compounds on the surface of the materials. Furthermore, Figure 10c reveals an additional band at 1630 cm^{-1} in the NO_2 spectrum of PD-MAPS_2 that can be assigned to the formation of nitro compounds during NO_2 adsorption.[16,40] The appearance of a new band in the NO_2 spectrum of PD-DMAPS_2 (Figure 10d) at 3100 cm^{-1} was observed as well.

The corresponding FT-IR spectra of the same materials are presented in Figure 11. The FT-IR spectra for all four samples clearly show the appearance of a new band at 690 cm^{-1} that can be attributed to the S—O stretching vibrations in accordance with the FT-Raman spectra shown in Figure 10. Also, the SO_2-treated materials showed decreased IR band intensities in their IR spectra. Moreover, the peaks in the range 1450−1600 cm^{-1} can be associated with C—N stretches, whereas the bands in the range 3300−3700 cm^{-1} are assigned to NH and NH_2 stretching modes, along with modes associated with OH species. As with the FT-Raman data, none of the FT-IR spectra revealed any distinct change in the chemical structure of the materials after exposure to NO. In the spectra of the materials after exposure to NO_2, a new strong band was observed at ca. 1384 cm^{-1} for all of these adsorbents that corresponds to N═O asymmetric stretching mode of nitrate compounds as a result of NO_2 adsorption. From the comparison of the FT-IR spectra of the fresh and NO_2-treated materials in Figure 11, it can be seen that some bands in the 1450−1600 cm^{-1} region diminished after NO_2 exposure, suggesting that NO_2 might have reacted with amine groups, therebyb degrading the amine functionality. This is consistent with the results shown in section 3.2.6 and could explain the significant loss in CO_2 capacity after NO_2 exposure. However, it should be noted that the FT-IR spectra (as well as the FT-Raman spectra) were not obtained under rigorously quantitative conditions, and the spectra should therefore be viewed qualitatively.

4. CONCLUSIONS

The stabilities of several aminosilica adsorbent materials used for CO_2 capture (classified as class 1 and class 2 adsorbents) were studied in the presence of SO_2, NO, and NO_2. Under the experimental conditions studied here, the secondary amines adsorbed more SO_2 than the primary and tertiary amines with comparable amine loadings and exhibited more stability after SO_2 treatment by displaying higher normalized CO_2 capacities. The compiled data for the SO_2 adsorption experiments suggest that, for similar amine loadings, the MAPS-grafted silica adsorbents containing only secondary amines presented the highest affinity toward SO_2. The primary amines were found to adsorb NO much more than their secondary and tertiary

dx.doi.org/10.1021/ie4019116 | Ind. Eng. Chem. Res. 2013, 52, 12192−12201

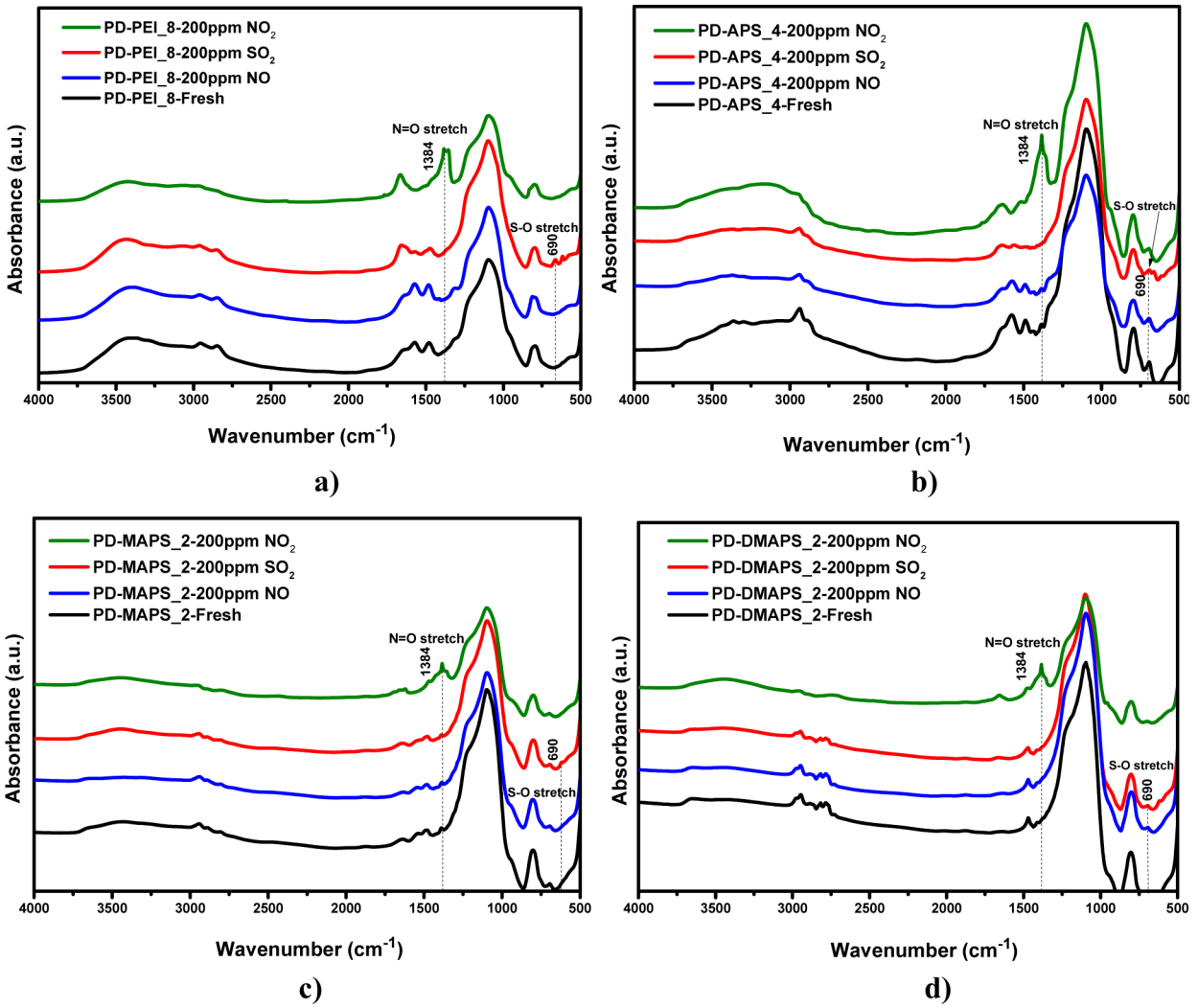

Figure 11. FT-IR spectra of (a) PEI, (b) APS, (c) MAPS, and (d) DMAPS before and after exposure to 200 ppm SO_2, NO_2, and NO at 35 °C.

counterparts when the amine loading was high, but overall, the affinity of all supported amine adsorbents toward NO was low. On the contrary, whereas the silica-supported materials were exceedingly resistant to NO, under the same conditions, all materials displayed very large NO_2 uptakes, and as a result, their CO_2 capacities dropped dramatically after exposure. On the basis of our experimental results, it can be inferred that NO_2 binds irreversibly to the amino groups and, hence, causes a significant loss in CO_2 adsorption capacity. To assess any synergies in the coadsorption of CO_2 and SO_2 or NO_x gases, a series of dynamic coadsorption experiments will be the focus of a future report.

AUTHOR INFORMATION

Corresponding Author

*E-mail: cjones@chbe.gatech.edu.

Notes

The authors declare no competing financial interest.

ACKNOWLEDGMENTS

This work was financially supported by DOE-NETL through Grant DE-FE0007804. However, any opinions, findings, conclusions, or recommendations expressed herein are those of the author(s) and do not necessarily reflect the views of the DOE.

REFERENCES

(1) Haszeldine, R. S. Carbon Capture and Storage: How Green Can Black Be? *Science* **2009**, *325*, 1647.

(2) Rochelle, G. T. Amine Scrubbing for CO_2 Capture. *Science* **2009**, *325*, 1652.

(3) Choi, S.; Drese, J. H.; Jones, C. W. Adsorbent Materials for Carbon Dioxide Capture from Large Anthropogenic Point Sources. *ChemSusChem* **2009**, *2*, 796.

(4) Hedin, N.; Andersson, L.; Bergström, L.; Yan, J. Adsorbents for the Post-Combustion Capture of CO_2 Using Rapid Temperature Swing or Vacuum Swing Adsorption. *Appl. Energy* **2013**, *104*, 418.

(5) It should be noted that adsorbents overloaded with amines to try to achieve high equilibrium capacities will be disadvantaged by slow adsorption/desorption kinetics.[6−8]

(6) Qi, G.; Wang, Y.; Estevez, L.; Duan, X.; Anako, N.; Park, A.-H. A.; Li, W.; Jones, C. W.; Giannelis, E. P. High Efficiency Nanocomposite Sorbents for CO_2 Capture Based on Amine-Functionalized Mesoporous Capsules. *Energy Environ. Sci.* **2011**, *4*, 444.

(7) Bollini, P.; Brunelli, N. A.; Didas, S. A.; Jones, C. W. Dynamics of CO_2 Adsorption on Amine Adsorbents. 1. Impact of Heat Effect. *Ind. Eng. Chem. Res.* **2012**, *51*, 15145.

(8) Bollini, P.; Brunelli, N. A.; Didas, S. A.; Jones, C. W. Dynamics of CO_2 Adsorption on Amine Adsorbents. 2. Insights into Adsorbent Design. *Ind. Eng. Chem. Res.* **2012**, *51*, 15153.
(9) Bollini, P.; Didas, S. A.; Jones, C. W. Amine-Oxide Hybrid Materials for Acid Gas Separations. *J. Mater. Chem.* **2011**, *21*, 15100.
(10) Li, W.; Drese, J. H.; Choi, S.; Hornbostel, M.; Krishnan, G.; Eisenberger, P. J.; Jones, C. W. Steam-Stripping for Regeneration of Supported Amine-Based CO_2 Adsorbents. *ChemSusChem* **2010**, *3*, 899.
(11) Most of the studies concerning CO_2 capture have focused on testing under idealized flue gas conditions, taking into account CO_2 and N_2 components only while neglecting other important constituents such as O_2,[12−15] water, CO, SO_x,[16−18] NO_x,[16,18−20] and particulates.
(12) Belmabkhout, Y.; Serna-Guerrero, R.; Sayari, A. Amine-Bearing Mesoporous Silica for CO_2 Removal from Dry and Humid Air. *Chem. Eng. Sci.* **2010**, *65*, 3695.
(13) Belmabkhout, Y.; Serna-Guerrero, R.; Sayari, A. Adsorption of CO_2-Containing Gas Mixtures over Amine-Bearing Pore-Expanded MCM-41 Silica: Application for Gas Purification. *Ind. Eng. Chem. Res.* **2010**, *49*, 359.
(14) Li, W.; Bollini, P.; Didas, S. A.; Choi, S.; Drese, J. H.; Jones, C. W. Structural Changes of Silica Mesocellular Foam Supported Amine-Functionalized CO_2 Adsorbents upon Exposure to Steam. *ACS Appl. Mater. Interfaces* **2010**, *2*, 3363.
(15) Bollini, P.; Choi, S.; Drese, J. H.; Jones, C. W. Oxidative Degradation of Aminosilica Adsorbents Relevant to Postcombustion CO_2 Capture. *Energy Fuels* **2011**, *25*, 2416.
(16) Diaf, A.; Garcia, J. L.; Beckman, E. J. Thermally Reversible Polymeric Sorbents for Acid Gases: CO_2, SO_2, and NO_x. *J. Appl. Polym. Sci.* **1994**, *53*, 857.
(17) Khatri, R. A.; Chuang, S. S. C.; Soong, Y.; Gray, M. Thermal and Chemical Stability of Regenerable Solid Amine Sorbent for CO_2 Capture. *Energy Fuels* **2006**, *20*, 1514.
(18) Diaf, A.; Beckman, E. J. Thermally Reversible Polymeric Sorbents for Acid Gases, IV. Affinity Tuning for the Selective Dry Sorption of NO_x. *React. Polym.* **1995**, *25*, 89.
(19) Xu, X.; Song, C.; Miller, B. G.; Scaroni, A. W. Adsorption Separation of Carbon Dioxide from Flue Gas of Natural Gas-Fired Boiler by a Novel Nanoporous "Molecular Basket" Adsorbent. *Fuel Process. Technol.* **2005**, *86*, 1457.
(20) Liu, Y.; Ye, Q.; Shen, M.; Shi, J.; Chen, J.; Pan, H.; Shi, Y. Carbon Dioxide Capture by Functionalized Solid Amine Sorbents with Simulated Flue Gas Conditions. *Environ. Sci. Technol.* **2011**, *45*, 5710.
(21) Yagi, T.; Shibuya, H.; Sasaki, T. Application of Chemical Absorption Process to CO_2 Recovery from Flue Gas Generated in Power Plants. *Energy Convers. Manage.* **1992**, *33*, 349.
(22) Aaron, D.; Tsouris, C. Separation of CO_2 from Flue Gas: A Review. *Sep. Sci. Technol.* **2005**, *40*, 321.
(23) Uyanga, I. J.; Idem, R. O. Studies of SO_2- and O_2-Induced Degradation of Aqueous MEA during CO_2 Capture from Power Plant Flue Gas Streams. *Ind. Eng. Chem. Res.* **2007**, *46*, 2558.
(24) Belmabkhout, Y.; Sayari, A. Isothermal versus Non-isothermal Adsorption−Desorption Cycling of Triamine-Grafted Pore-Expanded MCM-41 Mesoporous Silica for CO_2 Capture from Flue Gas. *Energy Fuels* **2010**, *24*, 5273.
(25) Li, G.; Xiao, P.; Webley, P.; Zhang, J.; Singh, R.; Marshall, M. Capture of CO_2 from High Humidity Flue Gas by Vacuum Swing Adsorption with Zeolite 13X. *Adsorption* **2008**, *14*, 415.
(26) Sultana, A.; Habermacher, D. D.; Kirschhock, C. E. A.; Martens, J. A. Adsorptive Separation of NO_x in Presence of SO_x from Gas Mixtures Simulating Lean Burn Engine Exhaust by Pressure Swing Process on Na−Y zeolite. *Appl. Catal. B: Environ.* **2004**, *48*, 65.
(27) Rouf, S. A.; Eic, M. Adsorption of SO_2 fromWet Mixtures on Hydrophobic Zeolites. *Adsorption* **1998**, *4*, 25.
(28) Perdana, I.; Creaser, D.; Öhrman, O.; Hedlund, J. A Comparison of NO_x Adsorption on Na, H and BaZSM-5 Films. *Appl. Catal. B: Environ.* **2007**, *72*, 82.
(29) Reddy, M. K. R.; Xu, Z. P.; Lu, G. Q. M.; Costa, J. C. D. Effect of SO_x Adsorption on Layered Double Hydroxides for CO_2 Capture. *Ind. Eng. Chem. Res.* **2008**, *47*, 7357.
(30) Lee, Y.; Kim, H.; Park, J.; Choi, B.; Choi, D.; Park, J. Adsorption and Reaction Behavior for the Simultaneous Adsorption of NO−NO_2 and SO_2 on Activated Carbon Impregnated with KOH. *Carbon* **2003**, *41*, 1881.
(31) Lu, H.; Smirniotis, P. G. Calcium Oxide Doped Sorbents for CO_2 Uptake in the Presence of SO_2 at High Temperatures. *Ind. Eng. Chem. Res.* **2009**, *48*, 5454.
(32) Ryu, H.; Grace, J. R.; Lim, C. J. Simultaneous CO_2/SO_2 Capture Characteristics of Three Limestones in a Fluidized-Bed Reactor. *Energy Fuels* **2006**, *20*, 1621.
(33) Sun, P.; Grace, J. R.; Lim, C. J.; Anthony, E. J. Removal of CO_2 by Calcium-Based Sorbents in the Presence of SO_2. *Energy Fuels* **2007**, *21*, 163.
(34) Ridha, F. N.; Manovic, V.; Macchi, A.; Anthony, E. J. The Effect of SO_2 on CO_2 Capture by CaO-Based Pellets Prepared with a Kaolin Derived $Al(OH)_3$ Binder. *Appl. Energy* **2012**, *92*, 415.
(35) Zhang, J.; Xiao, P.; Li, G.; Webley, P. A. Effect of Flue Gas Impurities on CO_2 Capture Performance from Flue Gas at Coal-Fired Power Stations by Vacuum Swing Adsorption. *Energy Proc.* **2009**, *1*, 1115.
(36) Lukens, W. W.; Schmidt-winkel, P.; Zhao, D.; Feng, J.; Stucky, G. D. Evaluating Pore Sizes in Mesoporous Materials: A Simplified Standard Adsorption Method and a Simplified Broekhoff−de Boer Method. *Langmuir* **1999**, *15*, 5403.
(37) Didas, S. A.; Kulkarni, A. R.; Sholl, D. S.; Jones, C. W. Role of Amine Structure on Carbon Dioxide Adsorption from Ultradilute Gas Streams such as Ambient Air. *ChemSusChem* **2012**, *5*, 2058.
(38) Barman, S.; Philip, L. Integrated System for the Treatment of Oxides of Nitrogen from Flue Gases. *Environ. Sci. Technol.* **2006**, *45*, 1035.
(39) Choi, S.; Drese, J. H.; Eisenberger, P. M.; Jones, C. W. Application of Amine-Tethered Solid Sorbents for Direct CO_2 Capture from the Ambient Air. *Environ. Sci. Technol.* **2011**, *45*, 2420.
(40) Levasseur, B.; Amani, M. E.; Bandosz, T. J. Interactions of NO_2 with Amine-Functionalized SBA-15: Effect of Synthesis Route. *Langmuir* **2011**, *28*, 5703.